

Study of Copper Corrosion Inhibition in an 3.5% NaCl Solution with Potassium-o-Ethyl Dithiocarbonate

H.Baeza, M.Guzman*, R.Lara

Departamento de Química, Facultad de Ciencias, Universidad Católica del Norte, Antofagasta-Chile.

*E-mail: mguzman@ucn.cl

Received: 3 December 2012 / Accepted: 13 February 2013 / Published: 1 June 2013

Using the electrochemical polarization resistance technique, the inhibitor behavior of potassium-o-ethyl dithiocarbonate (potassium ethyl xanthate) is studied for copper in a 3.5 % NaCl aqueous solution. The inhibition mechanism is mixed, apparent activation energy with inhibitor being greater than without inhibitor. Experimental data fit Langmuir isotherm; the inhibitor is spontaneously adsorbed on the copper surface in an exothermic process. The inhibitor adsorption on the copper surface is physisorption.

Keywords: corrosion inhibition, adsorption isotherms, xanthate, potentiodynamic polarization, thermodynamic adsorption.

1. INTRODUCTION

Copper and its alloys are frequently used in industry because they have good electrical and thermal conductivity and also mechanical properties. Copper is resistant to corrosion in a neutral medium.

The literature describes several corrosion inhibitors of copper and its alloys. There are inorganic and organic inhibitors, the latter being quite numerous.

In general, some organic compounds have shown great effectiveness for inhibiting aqueous corrosion in a great variety of metals and alloys[1,2]. The adsorption of these metals is generally explained by the formation of a film on the metal surface. Inhibitor adsorption can prevent cathodic and anodic reactions or both. This inhibition may be a chemical or physical adsorption. This effect is obtained through the formation of a diffusion barrier or by blocking reaction sites[3,4]. Electrostatic attraction between the charged inhibitor molecule and the active charged sites on the metal surface results in physical adsorption. The literature shows that most organic inhibitors are adsorbed on the metal by surface water molecule displacement, forming a compact barrier[3]. Molecules containing

nitrogen and sulfur in their structures are good inhibitors, as compared to compounds that only contain sulfur or nitrogen[5]. The inhibition property of these compounds is attributed to their molecular structure. The planarity and pairs of free electrons in heteroatoms are important characteristics that determine the adsorption of these molecules on the metal surface". Heterocyclic compounds containing sulfur and nitrogen are good corrosion inhibitors in aggressive mediums[5-8]

The most common organic copper inhibitors are azoles[9], amines[10], amino acids[11], Triphenylmethane derivatives[12], thiole group compounds[8], and phosphates[13].

Xanthates have been used as collectors in the flotation of various copper sulfide minerals. Their efficiency as collectors is attributed to their interaction with mineral surface, probably through chemisorption. The xanthate adsorption on the copper surface may be associated with a hydrophilic / hydrophobic transition on the metal surface. The formation of the copper / xanthate layer shows interesting synergic effects on copper corrosion protection[14-18]. In Chile potassium-o-ethyl dithiocarbonate (potassium ethyl xanthate) is frequently used as a collector in copper mining. Since most copper producers are located in the northern region where water is scarce, the mineral is sometimes processed with sea water or water from wells with a high content of chloride, an ion known for its depassivating power. So, studying this system is quite interesting.

The purpose of this work is to study the corrosion inhibition of copper in a 3.5% NaCl solution when adding potassium-o-ethyl dithiocarbonate as inhibitor, apart from studying the kinetic aspects of inhibition and thermodynamic aspects of adsorption.

2. EXPERIMENTAL

2.1. Electrodes

The *work electrode* was built with 99.99% pure electrolytic copper. The copper was pretreated at 350°C in an inert environment during 15 minutes to eliminate tension. It was then slowly cooled at room temperature. The electrode consisted of a cylinder made of this iron, covered with epoxy resin and with a 0.50 cm² metal surface.

Before each experiment, the electrode was duly cleaned according to ASTM G1 standard. The cleaning method consisted in removing all impurities on the electrode surface, either oxide or epoxy resin. To do this, 3M 2000 wet sandpaper was used. The electrode was then submitted to a strong jet of tap water. The surface was brushed with liquid soap. Next, it was jet washed to thoroughly eliminate soap. Later, it was cleaned with deionized distilled water; Afterwards, it was washed with acetone. Finally, it was dried with adsorbent paper.

The *auxiliary electrode* or counter electrode made of platinum with a 1.77 cm² exposed surface was washed in a way similar to the work electrode.

The *reference electrode* was made of saturated calomelane. Before each measurement, it was washed with detergent, bidistilled water and dried with absorbent paper, the KCl solution being always saturated.

2.2. Medium.

The electrolytic medium was 99.9% pure Merck analytical grade sodium chloride, concentration being 3.5% for all the solutions. As corrosion inhibitor, 95% pure Merck potassium-o-ethyl dithiocarbonate (potassium ethyl xanthate) was used. It was purified with propanone. Figure 1 shows its structure. All the solutions were prepared with deionized bidistilled water.

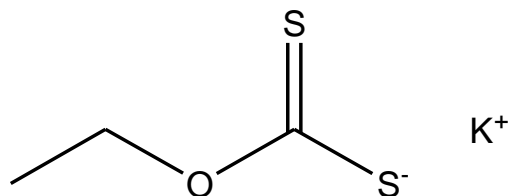


Figure1. Structure of potassium-o-ethyl dithiocarbonate

2.3. Measurement system

Once the work electrode was clean and dry, it was submerged into 50 mL of the solution to be tested during 30 minutes. After this period, the auxiliary and reference electrodes were introduced in a luggin probe, placing the capillary end at 2 to 3 mm from the work electrode surface.

Linear polarization curves were drawn by means of a Voltalab 40 Radiometer potentiostat using linear potentiometer techniques.

Polarization measures were taken with a 1 mVs^{-1} velocity. Temperatures (288.2; 293.3; 298.2; 303.2 and 308.2 K) of ($1 \times 10^{-4} \text{ M}$, $2 \times 10^{-4} \text{ M}$, $3 \times 10^{-4} \text{ M}$, $4 \times 10^{-4} \text{ M}$, $5 \times 10^{-4} \text{ M}$) inhibitor solutions were thermostated to $\pm 0.5^\circ\text{C}$ by means of a thermocirculator.

3. RESULTS AND DISCUSSION

The corrosion parameters obtained from polarization curves are shown in Table 1. Corrosion current density decreases as inhibitor concentration increases at different temperatures. The corrosion potential changes to more cathodic values as inhibitor concentration increases at different temperatures, which is consequent with the decrease of corrosion current density. Tafel slopes vary with inhibitor concentration at different temperatures, showing that this affects both the cathodic and anodic reaction. So, the inhibitor may be considered as acting with a mixed mechanism. At the same inhibitor concentration, performance decreases as temperature increases probably due to corrosion velocity increase with temperature and inhibitor adsorption decrease.

Efficiency was determined with the relation

$$\eta\% = \frac{[i_{\text{corr}} - i_{\text{corr}}(\text{inh})]}{i_{\text{corr}}} 100 \quad (\text{eq 1})$$

where $\eta\%$ is the inhibition percent, i_{corr} corrosion current density without inhibitor, and $i_{\text{corr}}(\text{inh})$ current density with inhibitor.

Table 1. Corrosion parameters derived from polarization curves

288.2 K						
Concentration mol dm ⁻³ x 10 ⁴	E _{corr} mV(SCE)	i _{corr} mA cm ⁻²	ba mV	-bc mV	η %	rate _{corr} mm y ⁻¹
Blank	-1600.1	0.6672	151.8	98.4	-	15.53
1	-1626.8	0.4823	153.0	95.1	27.71	11.23
2	-1631.6	0.4098	93.0	78.1	38.58	9.537
3	-1638.9	0.3594	72.9	64.7	46.13	8.364
4	-1667.4	0.3102	60.8	54.2	53.51	7.218
5	-1644.8	0.2787	53.2	49.2	58.23	6.487
293.2 K						
Blank	-1522.3	0.7211	297.9	177.1	-	16.79
1	-1593.6	0.5470	147.8	103.8	24.14	12.74
2	-1627.0	0.4565	138.3	93.4	36.69	10.62
3	-1627.9	0.3911	91.5	73.5	45.76	9.102
4	-1627.3	0.3477	64.5	62.4	51.78	8.093
5	-1653.2	0.3118	53.4	51.5	56.76	7.256
298.2 K						
Blank	-1510.4	0.8059	198.2	151.1	-	18.76
1	-1588.3	0.6189	214.0	128.2	23.20	14.41
2	-1597.5	0.5166	142.8	98.1	35.90	12.02
3	-1613.7	0.4543	96.5	79.0	43.63	10.58
4	-1687.6	0.4093	77.2	66.3	49.21	9.527
5	-1633.9	0.3661	55.3	55.9	54.57	8.522
303.2 K						
Blank	-1405.5	0.8818	391.5	192.8	-	20.53
1	-1573.6	0.7239	228.0	133.6	17.91	16.85
2	-1536.7	0.6035	133.8	104.9	31.56	14.05
3	-1600.0	0.5175	95.7	79.4	41.31	12.04
4	-1631.3	0.4680	95.2	75.3	46.93	10.89
5	-1613.9	0.4127	70.3	-64.9	53.20	9.571
308.2 K						
Blank	-1479.4	1.0576	279.2	188.6	-	24.62
1	-1568.0	0.8835	287.6	144.4	16.46	20.56
2	-1559.8	0.7440	178.6	117.5	29.65	17.32
3	-1573.9	0.6267	121.5	90.4	40.74	14.59
4	-1590.8	0.5703	109.8	82.6	46.08	13.27
5	-1591.6	0.5374	91.1	73.9	49.19	12.51

3.1. Kinetics

Temperature increase increases corrosion current density. The activation parameters of reaction kinetics with and without inhibitor can be calculated with the Arrhenius-type expression

$$i_{\text{corr}} = A e^{-\frac{E_a}{R T}} \tag{eq 2}$$

where i_{corr} is corrosion current density, A is Arrhenius pre-exponential factor, and E_a is apparent corrosion activation energy. Using data from the table above with or without inhibitor, at a $5 \cdot 10^{-4} \text{ mol dm}^{-3}$ concentration, we obtain Figure 2, where apparent activation energy without inhibitor is $16.52 \text{ kJ mol}^{-1}$, while it is $24.51 \text{ kJ mol}^{-1}$ with inhibitor. The increase of this energy in about 35% would indicate that corrosion becomes difficult when there is inhibitor. The difference remains when calculating other concentrations.

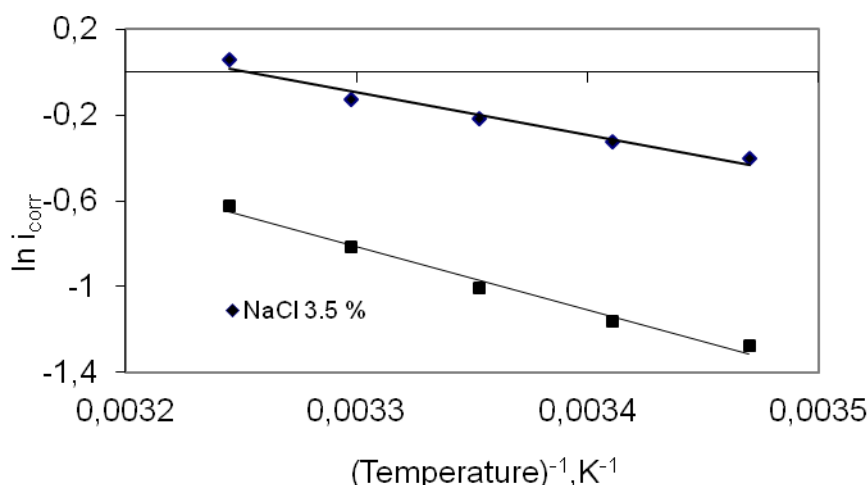


Figure 2. Arrhenius-type graph with or without $5 \cdot 10^{-4} \text{ M}$ inhibitor

3.2. Adsorption

Adsorption is described by means of an adsorption isotherm which provides the amount of adsorbate on the adsorbent as a function of the concentration at steady temperature.

In general, isotherms can be expressed as $Kc = \text{function}(\theta, f, x, h, n)$, where K^0 is normal adsorption equilibrium constant, c inhibitor concentration, θ the degree of covering by adsorbed molecules ($0 \leq \theta \leq 1$), x the number of water molecules displaced by an inhibitor molecules, f interaction factor among adsorbed molecules ($f < 0$ indicates repulsion force, $f > 0$ shows the lateral attraction among adsorbed organic molecules, h is a measure of adsorption energy distribution on various spots on the surface (this is an heterogeneity parameter ($0 \leq h \leq 1$)) and n is the number of spots occupied by the molecule adsorbed on the surface.

Many isotherms have been developed, some of them from theory and others from experimental data. Table 2 shows some of the most common isotherms [7,8].

Table 2. Adsorption isotherms

Author	Isotherm	Parameter
Langmuir	$K^{\circ}_c = \frac{\theta}{1-\theta}$	K°
Frumkin	$K^{\circ}_c = \left[\frac{\theta}{1-\theta} \right] \exp[-f\theta]$	K°, f
Hill-de Boer	$K^{\circ}_c = \left[\frac{\theta}{1-\theta} \right] \exp \left[\frac{\theta}{1-\theta} \right] \exp[-f\theta]$	K°, f
Parsons	$K^{\circ}_c = \left[\frac{\theta}{1-\theta} \right] \exp \left[\frac{2-\theta}{(1-\theta)^2} \right] \exp[-f\theta]$	K°, f
Temkin	$K^{\circ}_c = \theta \exp[-f\theta]$	K°, f
Langmuir-Freundlich	$K^{\circ}_c = \left[\frac{\theta}{(1-\theta)} \right]^{1/h}$	K°, h
Langmuir multistage	$K^{\circ}_c = \frac{\theta}{(1-\theta)^n}$	K°, n
Flory-Huggins	$K^{\circ}_c = \frac{\theta}{x(1-\theta)^{\chi}}$	K°, x
Dhar-Flory-Huggins	$K^{\circ}_c = \frac{\theta}{(1-\theta)^{\chi} \exp[\chi-1]}$	K°, x
Bockris-Swinkels	$K^{\circ}_c = \frac{\theta}{(1-\theta)^{\chi}} \frac{[\theta + \chi(1-\theta)]^{(\chi-1)}}{\chi^{\chi}}$	K°, x
Damaskin-Parsons	$K^{\circ}_c = \frac{\theta}{(1-\theta)^{\chi}} \exp[-f\theta]$	K°, x, f
Kastening-Holleck	$K^{\circ}_c = \frac{\theta}{x(1-\theta)^{\chi}} \left[1 - \theta + \frac{\theta}{x} \right]^{\chi-1} \exp[-f\theta]$	K°, x, f

The extent of coating of copper surface with inhibitor θ corresponds to the efficiency percent divided by 100.

Experimental data were tested in isotherms on Table 2, Langmuir isotherm being the one that best fits experimental data, with a coefficient correlation greater than 0.99 for all temperatures.

Langmuir isotherm is based on the fact that the adsorbent surface is uniform, that is, all adsorption spots are equivalent. Adsorbed molecules do not interact. An adsorbent molecule displaces a water molecule from the adsorbent surface. There is one-layer adsorption, that is, for $n=x=h=1$ and $f=0$ values, the isotherms in Table 2 are Langmuir isotherms, except Hill-de-Boer and Parson isotherms.

$$\frac{\theta}{1-\theta} = K^{\circ}_{ads} c \tag{eq 3}$$

where K_{ads}° corresponds to normal adsorption constant, c is inhibitor concentration, and θ the degree of covering. Considering ($\theta=0, c=0$), Table 3 shows K_{ads}° values which lower as temperature increases, thus indicating that the adsorption process is exothermic.

Table 3. Adsorption constant variation with temperature

Temperature, K	$K_{ads}^{\circ}, dm^3 mol^{-1}$
288.2	2870
293.2	2703
298.2	2477
303.2	2268
308.2	2066

To confirm that Langmuir isotherm fits experimental data better:

Covering coefficients were calculated with Langmuir equation, for example at 303.2 K and compared with the experimental one shown in Figure 3. This figure shows good agreement between experimental and calculated values.

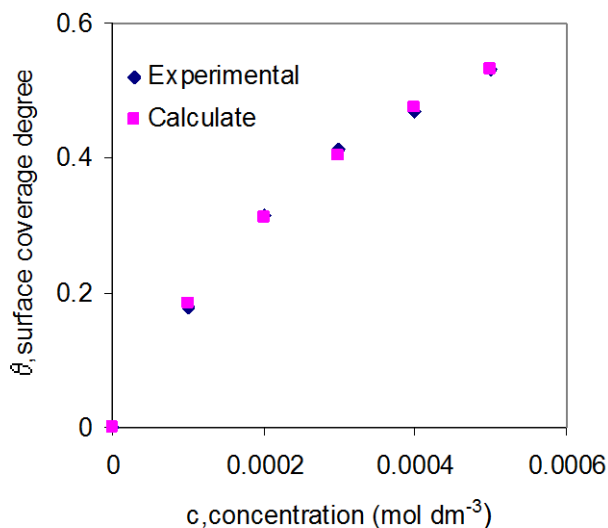


Figure 3. Comparison between experimental and calculated values of θ at 303.2K

The slope $\frac{d \log c}{d \theta} = \frac{1}{\log 10} \left[\frac{1}{(1-\theta)\theta} \right]$ corresponding to Langmuir isotherm in Figure 4 shows

slope curves at different temperatures versus the degree of covering, the minimum being close to $\theta=0.5$, corresponding to the isotherm inflection point. This value indicates that experimental data fit Langmuir isotherm¹⁹.

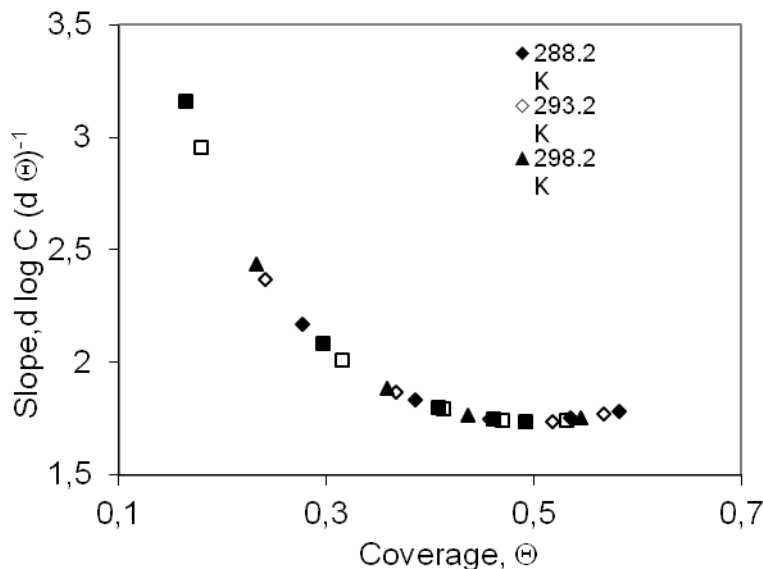


Figure 4. Slope versus inhibitor coating at different temperatures

3.3. Thermodynamic Adsorption Functions

According to Langmuir isotherm theory, an inhibitor molecule substitutes a water molecule on the metal surface during the adsorption process.

$H_2O_{ads} + Inhibitor_{sol} \rightleftharpoons H_2O_{sol} + Inhibitor_{ads}$ the normal equilibrium constant is

$$K_{ads}^{\circ} = \frac{|H_2O_{sol}| |Inhibitor_{ads}|}{|H_2O_{ads}| |Inhibitor_{sol}|} = e^{-\frac{\Delta G_{ads}^0}{R T}}, \frac{|Inhibitor_{ads}|}{|H_2O_{ads}|} = \frac{|Inhibitor_{sol}|}{|H_2O_{sol}|} e^{-\frac{\Delta G_{ads}^0}{R T}}$$

Langmuir $\frac{\theta_{inh}}{1 - \theta_{inh}} = K_{ads}^{\circ} |Inhibitor_{sol}| = \frac{|Inhibitor_{ads}|}{|H_2O_{ads}|} = \frac{|Inhibitor_{sol}|}{|H_2O_{sol}|} e^{-\frac{\Delta G_{ads}^0}{R T}}$ then,

$$K_{ads}^{\circ} = \frac{1}{|H_2O_{sol}|} e^{-\frac{\Delta G_{ads}^0}{R T}}, \text{ as water concentration at room temperature is about } 55.55 \text{ mol dm}^{-3}$$

³, then $K_{ads}^{\circ} 55.55 \text{ mol dm}^{-3} = e^{-\frac{\Delta G_{ads}^0}{R T}}$ thus,

$$\Delta G_{ads}^{\circ} = - R T \ln \left(K_{ads}^{\circ} 55,55 \right) \tag{eq 4}$$

Table 4 shows the values of normal adsorption energy variation at different temperatures. The table also shows that the normal free adsorption energy variation decreases as temperature increases. The negative sign indicates a spontaneous adsorption process. They found that calculated Gibbs energy

of adsorption values -29 to -33 kJ/mol the adsorption was regarded as physisorption, due to the electrostatic interaction the charged molecules and the charged metal[20-21].

Table 4. Normal free adsorption energy variation at different temperatures

Temperature, K	$\Delta G_{ads}^{\circ}, J mol^{-1}$
288.2	-28704
293.2	-29056
298.2	-29335
303.2	-29604
308.2	-29853

In plotting data from table 5 into Figure 5, a polynomial behavior can be observed with a correlation coefficient very close to a unit. Then, the normal free adsorption energy variation as a function of absolute temperature is given by

$$\Delta G_{ads}^{\circ} = 9.78546 \cdot 10^{-5} - 9.6848 \cdot 10^3 T + 3.2226 \cdot 10 T^2 - 3.5333 \cdot 10^{-2} T^3 J mol^{-1} \tag{eq5}$$

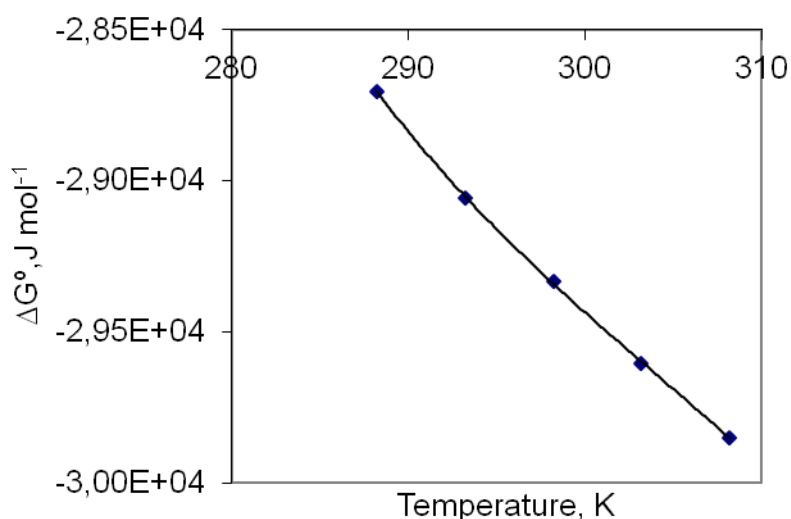


Figure 5. Normal free adsorption energy variation with temperature

Since $\left(\frac{\partial \Delta G_{ads}^{\circ}}{\partial T}\right)_P = -\Delta S_{ads}^{\circ}$, we have that for normal free adsorption entropy variation

$$\Delta S_{ads}^{\circ} = 9.6848 \cdot 10^3 - 6.4452 \cdot 10 T + 1.0600 \cdot 10^{-1} T^2 J (mol K)^{-1} \tag{eq 6}$$

On the other hand, since $\Delta H_{\text{ads}}^{\circ} = \Delta G_{\text{ads}}^{\circ} + T\Delta S_{\text{ads}}^{\circ}$, normal adsorption enthalpy variation

$$\Delta H_{\text{ads}}^{\circ} = 9.78546 \cdot 10^5 - 3.2226 \cdot 10 T^2 + 7,06673 \cdot 10^{-2} T^3 \text{ J mol}^{-1}. \quad (\text{eq7})$$

Then, in the temperature range analyzed, $\Delta G_{\text{ads}}^{\circ} < 0$, $\Delta H_{\text{ads}}^{\circ} < 0$, $\Delta S_{\text{ads}}^{\circ} > 0$, thus indicating that the adsorption process is spontaneous and exothermic.

4. CONCLUSIONS

Potassium-o-ethyl dithiocarbonate is a good indicator of copper corrosion in a 3.5% NaCl solution.

Inhibitor efficiency increases with concentration at any temperature.

The inhibitor mechanism acts on the cathodic and anodic reactions, so its action is mixed.

The activation energy of inhibitor corrosion with inhibitor is greater than without inhibitor.

Inhibitor adsorption on the copper surface fits Langmuir isotherm better.

In this case, the adsorption process is classified as physisorption.

The adsorption process is spontaneous and exothermic.

ACKNOWLEDGEMENTS

Authors thank the Master Program in Chemistry at Universidad Católica del Norte for its economic support. They also thank CONICYT for the scholarship granted to Magister H B.

References

1. V.S. Sastri. "Corrosion Inhibitors-Principles and Applications", John Wiley and Sons, Chichester, 1998.
2. V.S. Sastri, J.R Perumareddi, *Corrosion*, 53 (1997) 617
3. M. Elayyachy, A.El Idrissi, B.Hammouti, *Corros. Sci.*, 48 (2006) 2470
4. Abd-El-Nabey, E.Khamis, M.Sh. Radaman, A.El-Gindy, *Corrosion*, 52 (2000) 671
5. F.Bentiss, M. Lebrini, M.Lagrenée, *Corros. Sci.*, 47 (2005) 2915
6. M.Abdallah, E.A. Helal, A.S. Fouda, *Corros. Sci.*, 48 (2006) 1639
7. M. Guzman, R. Lara and L. Vera, *J. Chil. Chem. Soc.*, 54 (2009) 123
8. H. Baeza, M. Guzman, P. Ortega and L. Vera, *J. Chil. Chem. Soc.*, 48 (2003) 23
9. E. Sherif, A.Shamy, M. Ramla and A.Nazhawy, *Mater. Chem. Phys.*, 102 (2007) 231
10. E.Sheif and S.Park, *Electrochim. Acta*, 51 (2006) 4685
11. G.Moretti and F.Guidi, *Corros. Sci.*, 44 (2002) 1995
12. J.Polo, P.Pinilla, E.Cano and J.Bastidas, *Corrosion*, 59 (2003) 414
13. M.Edwards, L.Hidmi and D.Gladwell, *Corros. Sci.*, 44 (2002) 1057
14. S.González, M.Laz, R.Souto, R.Salvarezza and A.Arvia, *Corrosion*, 49 (1993) 450
15. J.Gómez, R.Salvarezza and A.Arvia, *J.Appl.Electrochem*, 17 (1987) 779
16. R.Souto, V. Fox, M.Perez, M. Laz and S.González, *Materials Science Forum* 19 (1995) 385
17. M.Scendo, *Corros. Sci.*, 47 (2005) 2778
18. M.Scendo, *Corros. Sci.*, 47 (2005) 1738
19. E. Cano, J.L. Polo, A. L.A Iglesia and J.M. Bastidas, *Adsorption*, 10 (2004) 219

20. M.A.Amin,S.S.Abd El Rehim,H.T.M.Abdel-Fatah, *Corros. Sci.* , 51 (2009) 882
21. G.Avci, *Mater.Chem.Phys.*112 (2008) 234

© 2013 by ESG (www.electrochemsci.org)